Parasites & Vectors

RESEARCH

Open Access

New insights into the molecular phylogeny, biogeographical history, and diversification of *Amblyomma* ticks (Acari: Ixodidae) based on mitogenomes and nuclear sequences

Juan E. Uribe[1,2*], Samuel Kelava[3], Santiago Nava[4], Andrea P. Cotes-Perdomo[5], Lyda R. Castro[6], Fredy A. Rivera-Paéz[7], Silvia Perea[1], Ben J. Mans[8,9], Alexander Gofton[10], Ernest J. M. Teo[3], Rafael Zardoya[1] and Stephen C. Barker[3]

Abstract

Background *Amblyomma* is the third most diversified genus of Ixodidae that is distributed across the Indomalayan, Afrotropical, Australasian (IAA), Nearctic and Neotropical biogeographic ecoregions, reaching in the Neotropic its highest diversity. There have been hints in previously published phylogenetic trees from mitochondrial genome, nuclear rRNA, from combinations of both and morphology that the Australasian *Amblyomma* or the Australasian *Amblyomma* plus the *Amblyomma* species from the southern cone of South America, might be sister-group to the *Amblyomma* of the rest of the world. However, a stable phylogenetic framework of *Amblyomma* for a better understanding of the biogeographic patterns underpinning its diversification is lacking.

Methods We used genomic techniques to sequence complete and nearly complete mitochondrial genomes –ca. 15 kbp– as well as the nuclear ribosomal cluster –ca. 8 kbp– for 17 *Amblyomma* ticks in order to study the phylogeny and biogeographic pattern of the genus *Amblyomma*, with particular emphasis on the Neotropical region. The new genomic information generated here together with genomic information available on 43 ticks (22 other *Amblyomma* species and 21 other hard ticks–as outgroup–) were used to perform probabilistic methods of phylogenetic and biogeographic inferences and time-tree estimation using biogeographic dates.

Results In the present paper, we present the strongest evidence yet that Australasian *Amblyomma* may indeed be the sister-group to the *Amblyomma* of the rest of the world (species that occur mainly in the Neotropical and Afrotropical zoogeographic regions). Our results showed that all *Amblyomma* subgenera (*Cernyomma*, *Anastosiella*, *Xiphiastor*, *Adenopleura*, *Aponomma* and *Dermiomma*) are not monophyletic, except for *Walkeriana* and *Amblyomma*. Likewise, our best biogeographic scenario supports the origin of *Amblyomma* and its posterior diversification in the southern hemisphere at 47.8 and 36.8 Mya, respectively. This diversification could be associated with the end of the connection of Australasia and Neotropical ecoregions by the Antarctic land bridge. Also, the biogeographic analyses let us see the colonization patterns of some neotropical *Amblyomma* species to the Nearctic.

*Correspondence:
Juan E. Uribe
juanuribearboleda@gmail.com
Full list of author information is available at the end of the article

Conclusions We found strong evidence that the main theater of diversification of *Amblyomma* was the southern hemisphere, potentially driven by the Antarctic Bridge's intermittent connection in the late Eocene. In addition, the subgeneric classification of *Amblyomma* lacks evolutionary support. Future studies using denser taxonomic sampling may lead to new findings on the phylogenetic relationships and biogeographic history of *Amblyomma* genus.

Keywords Ixodidae, Metastriata, Hard ticks, Pathogen vectors, Mitogenomics, Time-tree

Background

Ticks (Arachnida: Ixodida) are highly specialized, blood-sucking ectoparasites of vertebrates [1]. They are one of the main pathogen vectors (bacteria, viruses and protozoa) in the world, causing a expansive range of infections and diseases (such as rickettsioses, Lyme disease, relapsing fever borrelioses, Crimean-Congo hemorrhagic fever, babesioses, among others), and are therefore of maximal economic and health importance [2–5]. The order Ixodida comprises approximately 970 living species that are classified into three families, Nuttalliellidae (monotypic), Argasidae, and Ixodidae [6, 7]. Ixodidae (hard ticks) is the most diversified one with 771 valid species that are classified into two groups, Prostriata (with a single genus, *Ixodes*) and Metastriata (including 14 extant genera plus two additional fossil genera, *Compluriscutula* and *Cornupalpatum* [6]). Within Metastriata, *Amblyomma* is the second most diversified genus (after *Haemaphysalis*), comprising 136 living species, which are widely distributed across the Indomalayan, Afrotropical, Australasian, Nearctic and Neotropical biogeographic regions, reaching its highest diversity in the Neotropics region (67 species) [8]. The wide distribution, high diversity, and economic and health importance make the genus *Amblyomma* a priority group for evolutionary and biogeographical studies.

For many years, the genera *Amblyomma* and *Aponomma* were grouped together in the subfamily Amblyomminae or in the subtribe Amblyommini [9, 10]. However, Dobson and Barker [11], using DNA sequencing, determined that the genus *Aponomma* was paraphyletic and, consequently, also the subfamily Amblyomminae. "Indigenous" and "primitive" *Aponomma* species sensu Kaufman [12] were recovered as independent lineages and assigned to their own genera, *Bothriocroton* [13], *Robertsicus* and *Archaeocroton* [14], while "typical" *Aponomma* species sensu Kaufman [12] were transferred to the *Amblyomma* genus [13]. Recently, *Amblyomma transversale* has emerged as an early and independent branch in the mitogenomic tree of Metastriata, and has been elevated to the genus level, namely *Africaniella* [15]. As a consequence of the numerous taxonomic changes in the group, the current *Amblyomma* diversity seems to retain plesiomorphic characters that make the taxonomic boundaries diffuse. This diffuse state also hinders the assignment of fossils to a given cladogenetic event for estimation of their ages of diversification. Likewise, the most robust evolutionary framework for these lineages (based on mitochrondrial [mt] genomes) is not complete enough to either establish potential diversification events or to explain the current wide tropical distribution of the Metastriata group [16].

Various studies have been conducted with the aim to understand the evolutionary patterns of the *Amblyomma* species and the potential historical events that have driven their diversification [16–28]. However, a robust phylogeny of the genus is still lacking. Additionally, the subgeneric classification of *Amblyomma* sensu Santos Dias [29] and Camicas et al. [30] (9 subgenera: *Adenopleura*, *Amblyomma*, *Anastosiella*, *Aponomma*, *Cernyomma*, *Dermiomma*, *Haemalastor*, *Walkeriana* and *Xiphiastor*) has shown to be particularly weak from a phylogenetic perspective [16–18, 31].

Hence, evolutionary studies of *Amblyomma* remain inconclusive although weakly supported available phylogenetic frameworks of the genus show that early divergences are restricted to species endemic of Australian and the southern Neotropical regions [23, 24, 26]. Furthermore, IAA (Indomalayan, Afrotropical and Australasian biogeographic ecoregion) species are recovered in a derived phylogenetic position, together with a wide polytomy across main American lineages [26]. Thus far, genomic sequence data and taxon sampling are sparse, precluding the existence of a robust biogeographical hypothesis for hard ticks, especially in the Neotropic region, where the highest diversity of *Amblyomma* (67 species) is found.

At present, 316 mt genomes are available for the order Ixodida (at August 2023; [16, 31, 32]), but these only cover 20 species of *Amblyomma*, far from representing the diversity of the genus, or at least its main lineages. Therefore, the aim of this study was to generate a balanced mitogenomic dataset to reconstruct, using probabilistic methods, a robust and stable phylogenetic framework of *Amblyomma* for a better understanding of the evolutionary history and the biogeographic patterns underpinning its diversification, with particular emphasis on the Neotropical region.

Methods

Sample collection, DNA extraction and sequencing

A total of 17 *Amblyomma* species were collected and processed in this study (see Additional file 1: Table S1 for a complete list, localities, collector and sampling date of each of these species). All samples were fixed in absolute ethanol and stored at - 20ºC. After morphological identification, total DNA was extracted using the Qiagen DNeasy Blood & Tissue Kit (Qiagen, Hilden, Germany) following the manufacturer's spin-column protocol.

Using universal primers [33], we amplified the partial fragment of mt cytochrome *c* oxidase I (COXI) by PCR and performed Sanger sequencing with the aim of molecular re-confirmation. The mt genomes of five species were subjected to long-range PCR amplification using specific primers based on the partial COX1 fragment and conserved regions using the reaction contents and thermocycler conditions described by Cotes-Perdomo et al. [28]. The long-range PCR products were purified by ethanol precipitation, and cleaned fragments from the same mt genome were pooled together in equimolar concentrations, followed by shearing to an average fragment size of 450 bp using the Covaris ME220 Focused-ultrasonicator (Covaris, Woburn, MA, USA). The library preparation and massive parallel sequencing protocol were performed at the Laboratories of Analytical Biology (LAB-NMNH) as described in Uribe et al. [25]. For each remaining sample, a TruSeq Nano DNA Library was constructed and subjected to whole-genome sequencing (WGS) on the NovaSeq 6000 platform (150PE, 18 Gb/ea; Macrogen®, Seoul, Korea). The sequencing methods of the samples are described in Additional file 1: Table S1, and the primers and amplification strategy are described in Additional file 2: Table S2.

Data curation and ortholog search

Three types of massive parallel sequencing were combined in this study, namely amplicons, WGS and RNA sequencing (RNA-Seq) (available in NCBI; see Additional file 1: Table S1), for the configuration of the matrices. The quality of the massive sequencing was assessed using FastQC version 0.10.1 [34]. All raw reads were trimmed and cropped, and adapters were removed using Trimmomatic version 0.39 [35]. Paired-end cleaned reads were *de novo* assembled with SPAdes version 3.14.0, using spades.py [36] and rnaspades.py [37]. For the amplicon sequencing and WGS, the assembled mt genomes for each species were filtered by BLAST version 2.6.0 [38] searching against a custom database created using all *Amblyomma* mt genomes available. Then, the previously sequenced COX1 of each sample was used to corroborate the identifications. All individualized mt genomes were reference mapped using the paired-end cleaned reads with Geneious® in order to visually check the assemblies and determine the mean depth coverage. Mitochondrial elements were annotated using MITOS [39] and the open reading frames (ORFs) were manually checked. The boundaries of ribosomal genes were determined following Boore et al. [40].

Construction of matrices and phylogenetic inferences

A total of 60 mt genomes (including 17 new mt genomes of *Amblyomma*) were used to construct matrices, where three *Ixodes* species were used as outgroup of Metastriata. The complete list of matrices and their features are shown in Additional file 3: Table S3. The protein-coding genes were aligned using nucleotide sequences guided by the deduced amino acids in the Translator X server [41] with MAFFT v5 [42]. The nucleotide sequences of both ribosomal RNA (rRNA) genes were aligned using MAFFT version 7 [43] with default parameters. Additionally, a nuclear matrix was contracted using the ribosomal cluster for 12 *Amblyomma* species that represent all biogeographic regions.

Phylogenetic relationships were inferred using maximum likelihood (ML; [44]) and Bayesian inference (BI; [45, 46]). BI analyses were performed using two software programs: (i) under MrBayes v.3.1.2. [47], four simultaneous Markov chain Monte Carlo (MCMC) chains for 20 million generations were run, with sampling every 1000 simulated samples and discarding the first 25% as burn-in to prevent sampling before reaching stationarity; and (ii) under PhyloBayes [48], the site-heterogeneous model of evolution CAT-GTR model was selected [49], and two independent MCMC chains were run, with sampling every cycle, until convergence (checked a posteriori using the tools implemented in PhyloBayes; maximum difference < 0.1, maximum discrepancy < 0.1, effective sample size > 100). Consensus trees and the posterior probabilities (PP) of the nodes were obtained after discarding the first 10% cycles. The convergence of MCMC chains was checked and determined in Tracer v.1.7 [50]. ML analyses were carried out in IQ-TREE v.1.6.1 using a combination of rapid hill-climbing and stochastic perturbation methods. A total of 1000 ultrafast bootstrap pseudoreplicates were performed to assess robustness of the inferred trees, including the percentage of bootstrap (PB) of the nodes.

Two matrices were constructed, one at the amino acid codification and one at the nucleotide codification. For the concatenated amino acids matrix, the best-fit amino acid replacement matrices (Rmatrix) were selected under Bayesian Information Criterion (BIC; [51]) using the command '–m TEST' in ModelFinder [52]; the fit of adding empirical frequency profiles (mixture model) to the selected amino acid replacement matrices was then tested using the BIC and the command

'–mset Rmatrix+C10, Rmatrix+C20, Rmatrix+C30, Rmatrix+C40, Rmatrix+C50, Rmatrix+C60' in ModelFinder. The nucleotide matrix was analyzed, concatenated and partitioned (by codon position + 12S and 16S rRNA). The best evolutionary model for the concatenated matrix was selected with ModelFinder under BIC, and the '-m TESTNEW' command, while for the partitioned matrices, the command line was '-m TESTMERGEONLY' (which also infers the best scheme partition). All models and the scheme selected are described in Additional file 3: Table S3.

Time-tree estimation

The BEAST 2.6.6 program [53] was used to perform a Bayesian estimation of divergence times among *Amblyomma* species, based on the mt genome using protein coding + ribosomal genes at nucleotide codification (subset of Matrix BI-NT-GBlock-Partitioned; see Additional file 3: Table S3). An uncorrelated relaxed molecular clock was used to infer branch lengths and nodal ages. The tree topology was set based on topology 2 (see Additional file 5: Fig. S1b) using *Dermacentor*, *Hyalomma*, *Rhipicephalus* and *Rhipicentor* as outgroups. For the clock model, the lognormal relaxed-clock model was selected, which allows rates to vary among branches without any a priori assumption of autocorrelation between adjacent branches. For the tree prior, a Yule process of speciation was employed. ModelFinder was used as indicated above to select the best-fit partition and evolutionary models (Additional file 3: Table S3). The final Markov chain was run twice for 100 million generations, with sampling every 10,000 generations, and the first 10 million generations were discarded as part of the burn-in process, according to the convergence of chains checked with Tracer v. 1.7.1. The effective sample size of all the parameters was > 200.

For the time estimations, we used a phylogenetic scenario previously reconstructed (also inferred here) as a scaffold to include dates of biogeographic events [20, 22, 28]. The posterior distribution of the estimated divergence times was obtained by specifying four calibration points as priors, which are highlighted as follows.

1. A first calibration point was set for the divergence of *Am. americanum* + *Am. cajennense* group, at between 25 and 15.2 million years ago (Mya), with a mean of 20 Mya (normal distribution; 3 Sigma, 0.01 Offset; 95% height posterior density [HPD]) [20].
2. A second calibration point was set to *Am. cajennense* group radiation with a mean of 17 Mya (normal distribution; 0.3 Sigma, 0.001 Offset; 95% HPD) [22].
3. A third calibration point was set for the *Am. mixtum* (*Am. cajennense* + *Am. patinoi*) cladogenetic event, with a mean of 6 Mya (normal distribution; 0.6 Sigma, 0.001 Offset; 95% HPD between 5.01 and 6.99 Mya) [20].
4. A fourth calibration point was set for the divergences of the *Am. maculatum* + *Am. tigrinum* cladogenetic event at between 3.3 and 0.899 Mya, with a mean of 2.1 Mya (normal distribution; 0.73 Sigma; 95% HPD) [22].

Biogeographical analyses

The biogeographical history of the genus *Amblyomma* was reconstructed using BioGeoBEARS [54] implemented in R. Four biogeographical models implemented in BioGeoBears were evaluated: DEC (Dispersal-Extinction-Cladogenesis [55]) and DIVA+like, plus these two models considering the "j" parameter (founder-event speciation), DEC+J and DIVALIKE+J [54]. Accounting for founder-event speciation is relevant when considering organisms such as *Amblyomma* due to their great relevance as vectors and their potential distribution changes by climate change and anthropogenic pressure (but see Ree and Sanmartin [56] for j parameter criticism). Biogeographic models were compared using the corrected Akaike information criterion (AICc) to determine the best-fit biogeographic model on data and the effect of adding the "j" parameter on model performance. For biogeographic analyses, the distribution range was divided in five areas that were defined based on the distribution of the species included (Nearctic [NE], Neotropic [NO], Australia [AU], Afrotropic [AF] and Indomalayan [IN]). Given that the evolutionary relationships of Metastriate are not resolved, no area was assigned to the outgroup (see Additional file 4: Table S4). The broad geographic scope of this study justifies the consideration of such large areas for computational efficiency and to achieve the reconstruction of the biogeographical history of the whole genus *Amblyomma*.

Results and Discussion

Ticks are the second most important vectors of disease globally and potentially one of the most critical organisms to be studied in every biological field. Establishing a solid evolutionary framework of *Amblyomma* within the Metastriata context may be key to understanding the origin of the diversification of the genus. In this study, we used the leafier tree (in number of species) published recently [26] to select the species representatives of each main lineage. Thus, the molecular dataset generated here is described and, for the first time at the mitogenomic level, used to reconstruct *Amblyomma* phylogenetic relationships to assess previous hypotheses related to the origin and patterns of diversification of the genus.

Mitogenomic features

A total of 17 mt genomes (3 of which were partial) were newly sequenced in this study, increasing the mt genome catalog available for this tick group to 39 genomes (from 22). The sequencing methods applied here to determine the mt genomes (amplicon and WGS) allowed us to obtain a sequencing depth similar to that reached in related articles recently published [16, 28] (see depth coverage in Additional file 1: Table S1). The features of the new complete mt genomes described here fit with those already reported for other mt genomes of Metastriata [57], including the gene order (except for *Africaniella tranversale* [27]), length of the genomes/genes and the two characteristic control regions. Also, a general feature of the 37 genes (13 protein-coding genes, 22 tRNAs and two rRNAs) fit with most metazoan mt genomes [40].

Phylogeny of Amblyomma

To reconstruct the internal relationships of *Amblyomma*, we inferred 12 phylogenetic trees in this study, six at the nucleotide level and six at the amino acid level. All trees were summarized in Fig. 1, where the nodes that were not recovered in at least half of the trees with significant statistical support (node ≥ 0.95 PP/80 PB) were collapsed (see all topologies in Additional file 5: Fig. S1a–l). Also, dataset features, best-fit partition schemes and models, and log-likelihood values of all phylogenetic analyses are provided in Additional file 3: Table S3. *Amblyomma* was recovered as monophyletic in all analyses (Fig. 1, node 1) and as sister to a clade that includes (*Dermacentor* ((*Rhipicentor* (*Hyalomma* + *Rhipicephalus*))), as has been widely reported in previous phylogenies [27, 57].

All topologies but two (i.e. Topology 7 and 11) are congruent in the early cladogenetic events of *Amblyomma*. Topology 7 and 11 (see Additional file 5: Fig. S1g, k)

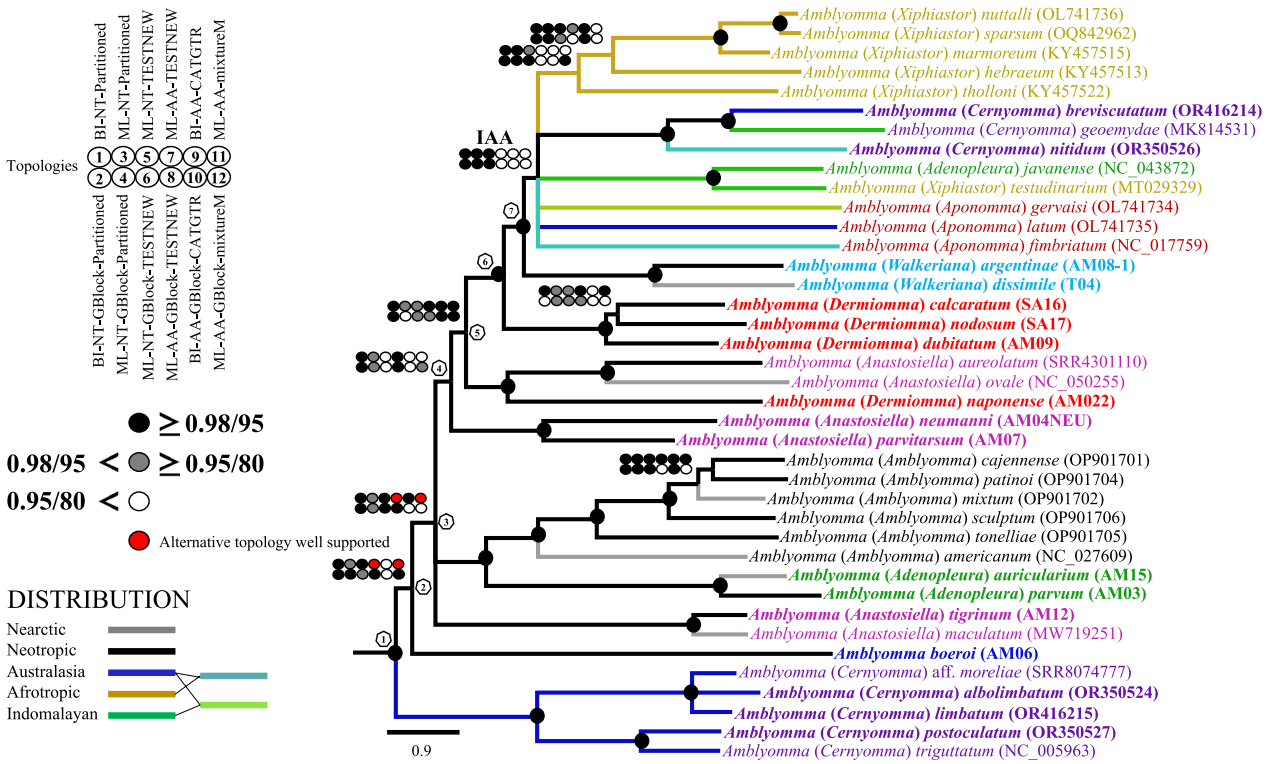

Fig. 1 Phylogenetic hypotheses for *Amblyomma* relationships based on the mitogenomic datasets. Two matrices were assessed using the coding protein genes at amino acid codification (AA) and at nucleotide codification (NT; this last includes both ribosomal genes). Trees were reconstructed using maximum-likelihood (ML) and Bayesian inference (BI) applying 6 treatments to each matrix (these are described in the left top of the figure and in section Methods section). Circles (left of tree) refer to the credibility support of the nodes, with the black-gilled circle indicating strong support; the gray-filled circle, moderate support; and the open circle, no significant support (at the left middle of figure). All trees were summarized based on the following criteria. If in at least half of the trees a given node is not recovered with significant statistical support (node ≥ 0.95 PP/80 PB), it is collapsed (see all topologies in Additional file 1: Fig. S1a–l). Black-filled circles at a given node indicate nodes with maximum bootstrap and PB values across the 12 inferences. The geographical distribution of the species included in the tree are indicated with color coding in their respective branches, as is described in the lets button. The scale bar is given in expected substitutions/site. The specimens sequenced in this study are highlighted in bold font, and species with the same subgeneric status are indicated in the same color. The lineage with Indomalayan, Afrotropical and Australasian distributions is indicated in the tree with IAA

recovered the *Am. maculatum* complex as a sister clade of *Amblyomma boeroi* with significant and moderate support. The rest of the trees recovered endemic Australian species as a sister clade of *Am. boeroi* (southern cone of South America) + the rest of *Amblyomma* lineages. No comparable results have been reached so far in the phylogenetic analyses (Fig. 1, node 2). Although Seabolt [23], Beati and Klompen [24], and Santodomingo et al. [26] recovered three endemic *Amblyomma* species from the southern cone of South America (*Am. boeroi*, *Am. parvitarsum* and *Am. neumanni*) and Australian endemic species as the first divergences of *Amblyomma*, these relationships differ between them. Beati and Klompen [24] recovered a sister-relationship between *Am. boeroi* and *Am. parvitarsum*, while Santodomigo et al. [26] and Seabolt [23] recovered *Am. neumanni* + *Am. parvitarsum* as a sister lineage of *Am. boeroi*, an endemic Australian clade in an early phylogenetic position, but without statistical support. In our analyses, *Am. neumanni* and *Am. parvitarsum* are recovered as sister species but in a derivative position with strong support (Fig. 1, node 4). The close phylogenetic relationship between *Am. parvitarsum* and *Am. neumanni* was previously reported [58]. *Amblyomma boeroi* was recovered as an independent phylogenetic lineage within the genus *Amblyomma*, but it shares some morphological characters with both *Am. parvitarsum* and *Am. neumanni* [19]. On the other hand, some endemic species of Australia were recovered as the first divergence, as sister clade of all other species of *Amblyomma* in all phylogenetic trees (Fig. 1). Our results are compatible with those from previous *Amblyomma* phylogenetic analyses (although they differ in some included endemic species of Australia) that recovered *Am. fimbriatum* and *Am. postoculatum* as the sister clade that includes *Am. moreliae*, *Am. albolimbatum* and *Am. limbatum* [24]. The species clustered in this Australian clade are mostly associated with reptile hosts, with the exception of *Am. postoculatum*, which parasitize the wallaby banded hare [59].

In node 3 (Fig. 1), a tripartite polytomy exists between the *Am. maculatum* group, which does not appear to be closely related to any other species included in our analyses (except in Topology 7 and 11, see above). Also in node 3, (*Am. parvum* + *Am. auricularium*) + (*Am. cajennense* group + *Am. americanum*) relationships are well supported. These relationships have been recovered in previous studies (clades G, H, I in [26]). The internal relationships within the *Am. cajennense* complex as well as its sister relationships with *Am. americanum* are congruent with previous phylogenetic analyses [20, 26, 28]; however, the related species to *Am. americanum* should be included in a mitogenomic framework to be discussed in future studies. Lastly, node 3 includes (*Am. neumanni* + *Am. parvitarsum*) + the remaining species, including Neotropical, Neotropical-Nearctic (as *Am. dissimile*) and IAA species.

In the clade that includes the remaining species of *Amblyomma*, successive relationships with strong support were recovered between nodes 5, 6 and 7 (Fig. 1), as follows:

((*Amblyomma aureolatum*, *Am. ovale*), *Am. naponense*) (Fig. 1). The close relationship between *Am. aureolatum* and *Am. ovale* was identified in previous studies [17, 25], as was that with *Am. naponense* (clade E [26, 60]). *Amblyomma aureolatum* and *Am. ovale* normally use members of order Carnivora as hosts for adult stages (despite both species having a more widespread range of hosts) and are morphologically similar. Both factors have led to confusion regarding their identification. *Amblyomma ovale* is more widely distributed (Nearctic and Neotropic) than *Am. aureolatum* (Neotropic) [8].

((*Amblyomma calcaratum*, *Am. nodosum*), *Am. dubitatum*) (Fig. 1). These relationships were previously recovered [26, 61, 62], but in our analyses the relationship of *Am. calcaratum* and *Am. nodosum* was not recovered in four of 12 trees. This is likely due to insufficient taxon sampling of the species related to this clade in our analyses, as *Am. yucumense* (normally associated to *Am. dubitatum*), *Am. hadanii* and *Am. coelebs* [26, 62]. Note that adults of *Am. nodosum* and *Am. calcaratum* have been often confused because they are normally associated with hosts in the Pilosa order (e.g. *Myrmecophaga tridactyla*, *Tamandua tetradactyla, T. mexicana*), although both have other hosts throughout their life-cycles [8].

((*Am. calcaratum*, *Am. nodosum*), *Am. dubitatum*) was recovered as sister linage of ((*Am. argentinae* + *Am. dissimile*) + the IAA species) with confident support in all topologies (node 6 and 7; Fig. 1). However, (*Am. argentinae* + *Am. dissimile*) as a sister clade of the IAA species was only recovered in the analyses with nucleotide codification (6 of out 12; Fig. 1). In the amino acid matrix, (*Am. argentinae* + *Am. dissimile*) appears in a wide polytomy with IAA species (see inset, Fig. 1). *Amblyomma argentinae* and *Am. dissimile* were recovered closely related to IAA species in a previous study but without statistical support [26]. The lack of taxonomic sampling may be the cause of the loss of the phylogenetic signal in this part of the phylogenetic assembly.

With regard to IAA species, three well-supported clades were recovered in our analyses: (i) (*Am. javanense* + *Am. testudinarium*), as was also recovered in

Uribe et al. [25]; (ii) the ((*Am. breviscutatum* + *Am. geoemydae*) *Am. nitidum*) clade, recovered for the first time with strong support in all topologies; *Am. geoemydae* and *Am. nitidum* have a Indomalayan distribution associated mostly to reptiles [63, 64], while *Am. breviscutatum* occurs in Australia and the southwestern Pacific on feral pigs and rats (as nymphs) [59, 65]; and (iii) the ((((*Am. nuttallli* + *Am. sparsum*) *Am. marmoreum*) *Am. hebraeum*) *Am. tholloni*) clade, which is well supported in seven out of 12 topologies (Fig. 1). This clade has also been reported in mitogenomic analyses [27, 66], it has an Afrotropical distribution and includes ticks with public health importance, as are the species of the marmoreum complex [66]. Finally, the increasing taxon sampling of the "typical" *Aponomma* forms (*Am. gervaisi, Am. latum* and *Am. fimbriatum*) supports the inclusion of these species in *Amblyomma* (see [13]) with strong statistical support, even though that their phylogenetic positions remain unresolved (Fig. 1).

The results of the present study are in agreement with those from previous analyses [16–18, 67], showing that most of the *Amblyomma* subgenera sensu Camicas et al. [67] and Santos Dias [29] are not monophyletic, as in the cases of *Cernyomma, Anastosiella, Xiphiastor, Adenopleura, Aponomma,* and *Dermiomma. Amblyomma* (as in [26, 28]) and *Walkeriana* were found to be the only monophyletic subgenera.

Finally, the nuclear tree (Additional file 6: Fig. S2) recovered a monophyletic *Amblyomma* but with a polytomy in its early relationships that involves *Am. boeroi*, *Am. postoculatum*, *Am. neumanni* + *Am. parvitarsum*, and a clade with the remaining *Amblyomma* species.

Origin of diversification and biogeographical history

Within Ixodidae, the recent incorporation in molecular phylogenetic analyses of *Africaniella transversale* and some species assigned previously to "*Aponomma*" have demonstrated that the morphological diversity of *Amblyomma* sensu stricto is due to the retention of plesiomorphic characters that mislead the circumscription of its living fauna [13–15] and potentially those of extinct fauna [68]. Thus, with the aim to evaluate an independent hypothesis of the origin and diversification of *Amblyomma* that is not linked to a potential bias related to the assignation of non-phylogenetically corroborated lineages, we used geographic dating from well-established phylogenetic frameworks of the *Am. cajennense* complex [20, 28] and *Am. parvum* [22] as an alternative to the taxonomic and phylogenetic unresolved questions of the genus.

The higher diversity of *Amblyomma* is displayed in the Neotropic region, which constitutes a biogeographic ecoregion extending from the center of Mexico to the southernmost point of South America, including the Caribbean Islands [69]. This region has a geological and paleoclimatic complex history given that mountain ranges with different origins converge, and several climatic fluctuations plus associated glaciations have occurred [70]. These circumstances have given rise to intricate scenarios that could explain the hyper diversity of the Neotropical region [71]. Additionally, this diversity could have been boosted by geological events through time, including: (i) continental drift [72, 73]; (ii) the intermittent connection through bridges, such as the Antarctic bridge that connected the southern cone of South America with the Australian Region [74, 75], and the Berigian bridge with a northern connection to the Palearctic Region [76]; and (iii) the complex geological dynamics in the northern Neotropical such as, for example, formation of the Isthmus of Tehuantepec and Panama [77–79].

Our new reconstructed time-calibrated tree dated the origin of *Amblyomma* at about 47.8 Mya, with a relatively short credibility interval (95% highest posterior density [HPD]: 57–39.6 Mya). This is the youngest origin estimated for *Amblyomma* so far, which controverts older estimations for the origin of the genus at 91 Mya [24], between the late Jurassic and Early Cretaceous [80], or at 89–77 Mya [23], as well of the Burmese amber fossils assigned to the genus (at 100 Mya [68, 81]). The inconsistencies of our results with previous works could be related to the representativeness of taxa and exclusive analyses of the mt genome. The absence of fossil calibrations may also result in an underestimation of divergence dates. Further work is needed to evaluate the time divergences of *Amblyomma* using solid topologies, perhaps including nuclear more information and calibrations of endemic species of islands (e.g., Galapagos, Hispaniola).

The origin of diversification of *Amblyomma* was estimated to have occurred 36.8 Mya (95% HPD: 43–31.6 Mya), an age that matches with the end of the Antarctic bridge connection of the southern hemisphere, in the Late Eocene, at about 35 Mya [74, 75]. The origin age of the diversification of the genus has been estimated at 74–60 Mya by Seabolt [23], which is close to the start of continental connections of the southern hemisphere at 65 Mya [74, 75]. Both scenarios do not rule out a Southern Hemisphere fauna connection. Additionally, our time-calibrated tree suggests an origin and posterior diversification of IAA lineages (positioned derivatives in Figs. 1, 2) between 24.6 and 23.3 Mya (95% HPD: 28.5–19.7 Mya).

We reconstructed the biogeographic patterns of *Amblyomma* with the time divergence framework. The ancestral area reconstructions under each evaluated biogeographical model were highly consistent (Fig. 3; Additional file 7: Fig. S3a–d; Additional file 4: Table S5). Nevertheless,

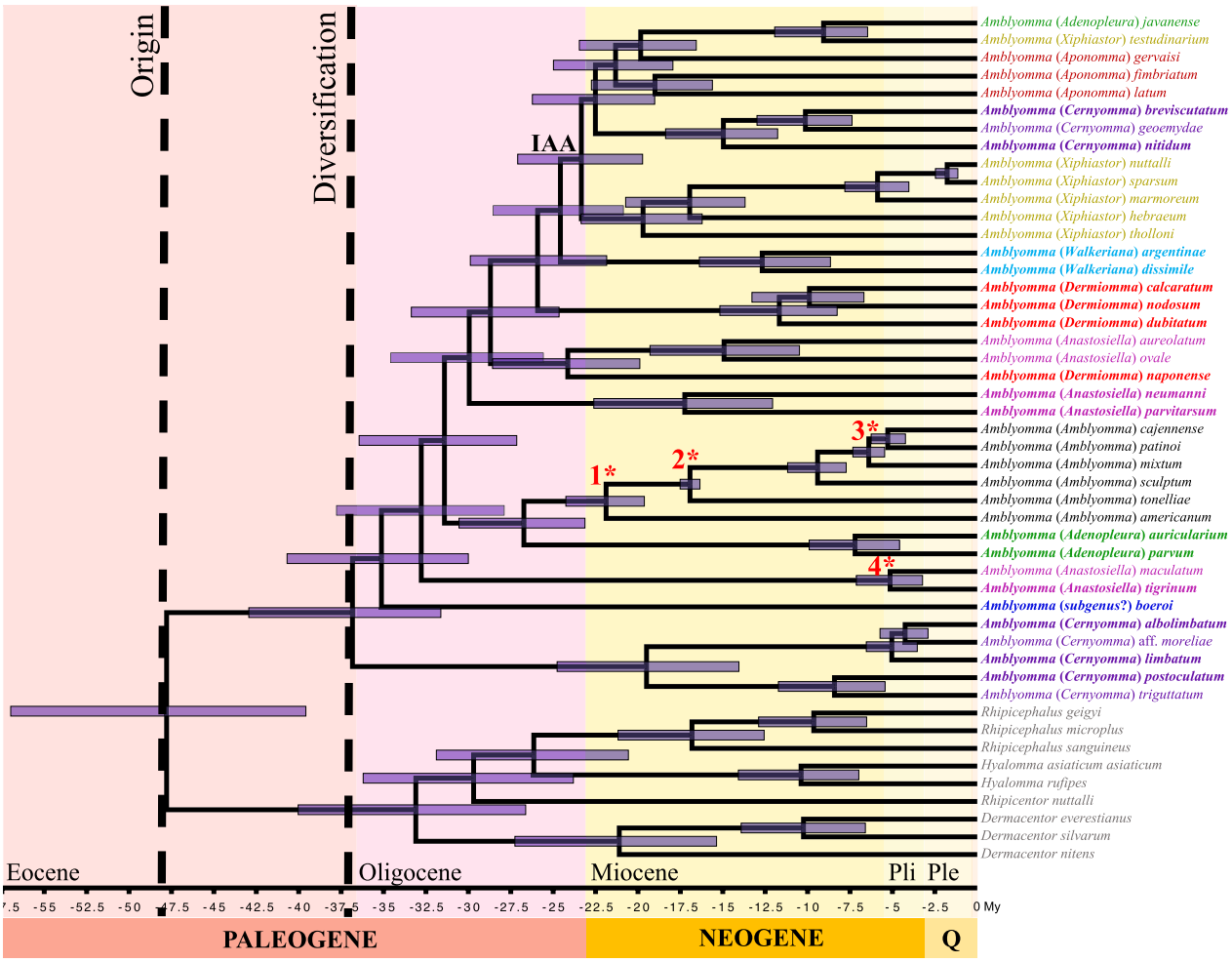

Fig. 2 Chronogram with age estimates of major divergence events among *Amblyomma* spp., based on the mitogenomic data set using Bayesian relaxed dating methods (BEAST) and topology 2 (Additional file 1: Fig. S1b). Horizontal bars represent 95% credibility intervals of relevant nodes, and the four calibration constraints are indicated in red with a number and asterisk on the corresponding nodes following the corresponding order date of the text. Dates (and credibility intervals) are in millions of years. Origin and diversification of *Amblyomma* are highlighted with a vertical broken line. Periods on the geological table are shown in different colors. The specimens sequenced in this study are highlighted in bold font. Species with the same subgeneric status are indicated in the same color. IAA, lineage with Indomalayan, Afrotropical, and Australasian distributions; My, million years; Ple, Pleistocene; Pli, Plicene; Q, Quaternary

models with the founder-event speciation parameter (j parameter, alternative hypothesis) outperformed those without it (null hypothesis) (DEC vs DEC+J, $P=0.0011$; DIVALIKE vs DIVALIKE+J, $p=0.007$). According to the log-likelihood (LnL) and AICc values, the DEC+J model was the best selected model (Additional file 4: Table S5) and, therefore, we have focused on reporting the results under this model. Our best biogeographic scenario supports the origin of the diversification of *Amblyomma* in the southern hemisphere at the end of the Eocene (Fig. 3), potentially associated with the faunistic flow in the final Antarctic Bridge connection [74, 75]. This scenario agrees with the South American and Australian lineages (here well represented) as the early diverging event in *Amblyomma* (Fig. 1) reached with high statistical support. This does not discard the hypothesis which argues that the origin of *Amblyomma* is in the Neotropic with a posterior colonization to Australia [24]. However, a solid phylogenomic framework of Metastriate (including main lineages of all genera) is necessary to evaluate the biogeographic patterns and ancestral distribution of the related lineages to *Amblyomma*, which could explain the Burmese amber fossil with a widespread ancestral distribution of the closest ancestors of *Amblyomma* [23, 68, 81]. Likewise, this could also make sense of an older origin of diversification of other lineages restricted to the

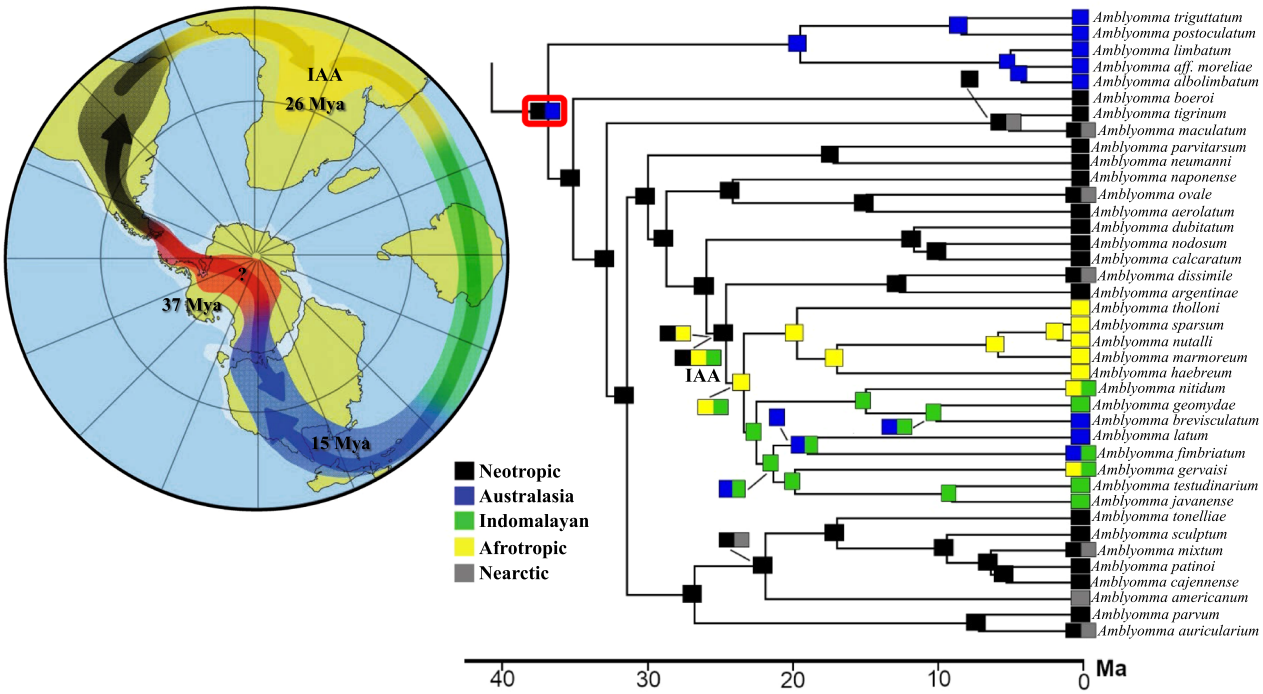

Fig. 3 Summary of the ancestral area reconstructions based on the time-tree calibrated (Fig. 2) with the five models used. Five stages were assessed, each of which is indicated with a different color. IAA indicates the lineage with Indomalayan, Afrotropical, and Australasian distributions. A graphic interpretation of the diversification patterns is included

early divergences of Metastriata, which have a notable Gondwanan distribution, as is the case of *Archaeocroton sphenodonti* (New Zealand), *Robertsicus elaphensis* (Nearctic), *Bothriocroton* (Australia) and *Africaniella transversale* (Afrotropic) [24].

While it is necessary to increase the representation of *Amblyomma* species in a phylogenomic framework, the biogeographic hypotheses proposed here support independent expansions along the Neocene to Quaternary era, as is the case of *Am. dissimile*, *Am. ovale* and *Am. auricularium* lineages. Also, our scenario supports a colonization event of *Am. americanum* and its related species (Fig. 3), despite these are not included in the present study.

Conclusions

Phylogenetic trees from mt genomes (Fig. 4 in [25]; [16]), nuclear rRNA (e.g. Fig. 5 in [16]; [26]; Fig. 8 in [27]), and from combinations of mt and nuclear rRNA genes and morphology [82] have hinted that the Australasian *Amblyomma* or the Australasian *Amblyomma* plus the *Amblyomma* species from South America might be the sister-group to the *Amblyomma* in the rest of the world. In the present study, however, we found the strongest evidence yet that Australasian *Amblyomma* may indeed be the sister-group to the *Amblyomma* of the rest of the world (Figs. 1, 3). The position of the Argentinian tick *Amblyomma boeroi* hints that the most recent common ancestor to the *Amblyomma* evolved in a region between South America and Australia, which would concur with the out-of-Antarctica hypothesis [24, 83]. Thus, on the one hand, the ancestor of the Australasian *Amblyomma* dispersed from Antarctica into that part of Gondwana which became Australasia, and on the other hand, the ancestor of the South American *Amblyomma* dispersed from Antarctic into that part of Gondwana which became South America. Our tree hypothesis also reveals that all *Amblyomma* subgenera included in our study, with the exception of *Walkeriana* and *Amblyomma*, are not monophyletic. Our findings suggest an origin of *Amblyomma* and its posterior diversification to be more recent than the previous hypotheses (47.8 and 36.8 Mya, respectively). Also, the biogeographic analyses reveal the colonization patterns of some neotropical *Amblyomma* species to the Nearctic. Finally, it has been well documented [84, 85] that increasing taxon sampling has a positive effect on tree reconstruction, resulting in more accurate topologies. Thus, future work should aim to reconstruct phylogenetic trees with a denser taxon sampling across both *Amblyomma* and Metastriate.

Supplementary Information

The online version contains supplementary material available at https://doi.org/10.1186/s13071-024-06131-w.

Additional file 1: Table S1. Complete list of the specimens used in this study with the respective GenBank accession number (#), localities, mt genome length, author reference and molecular strategy used. Asterisk indicates partial mt genomes.

Additional file 2: Table S2. Amplification strategy for mt genomes. The gene order of the mt genomes are indicated, where a gray color indicates the amplified and sequenced fragment of each species. The general and specific primers used are highlighted in yellow and red, respectively. The sequence of each primer is displayed in the 5′ to 3′ direction.

Additional file 3: Table S3. Dataset features, genetic codification, taxa included, best-fit partition schemes and models and log-likelihood (Ln likelihood) values of all phylogenetic analyses.

Additional file 4: Table S4. Presence (1) and absence (0) of the species included in the five biogeographic ecoregions assessed: Nearctic, Neotropic, Austral, Afrotropic, Indomalayan. **Table S5.** Report of statistical results across the four models implemented in BioGeoBear, including log-likelihood (LnL), number of parameters, f, e, j parameters and the Akaike information criterion (AICc) values.

Additional file 5: Figure S1. a Phylogenetic tree based on mt genome data: Topology 1 with 15 concatenated genes at nucleotide codification (protein-coding and ribosomal genes). Bayesian tree was reconstructed using the best fit evolutionary model and partition scheme. Numbers at nodes are statistical support values for bootstrap proportions. The scale bar is in expected substitutions/site. **b** Phylogenetic tree based on mt genome data: Topology 2 with 15 concatenated genes at nucleotide codification (protein-coding and ribosomal genes) implemented GBlock to trim the alignment. Bayesian tree was reconstructed using the best fit evolutionary model and partition scheme. Numbers at nodes are statistical support values for posterior probability. The scale bar is in expected substitutions/site. **c** Phylogenetic tree based on mt genome data: Topology 3 with 15 concatenated genes at nucleotide codification (protein-coding and ribosomal genes). Maximum-Likelihood tree was reconstructed using the best fit evolutionary model and partition scheme. Numbers at nodes are statistical support values for bootstrap proportions. The scale bar is in expected substitutions/site. **d** Phylogenetic tree based on mt genome data: Topology 4 with 15 concatenated genes at nucleotide codification (protein-coding and ribosomal genes) implemented GBlock to trim the alignment. Maximum-likelihood tree was reconstructed using the best fit evolutionary model and partition scheme. Numbers at nodes are statistical support values for bootstrap proportions. The scale bar is in expected substitutions/site. **e** Phylogenetic tree based on mt genome data: Topology 5 with 15 concatenated genes at nucleotide codification (protein-coding and ribosomal genes). Maximum-likelihood tree was reconstructed using the best fit evolutionary model for the concatenated matrix. Numbers at nodes are statistical support values for bootstrap proportions. The scale bar is in expected substitutions/site. **f** Phylogenetic tree based on mt genome data: Topology 6 with 15 concatenated genes at nucleotide codification (protein-coding and ribosomal genes) implemented GBlock to trim the alignment. Maximum-likelihood tree was reconstructed using the best fit evolutionary model for the concatenated matrix. Numbers at nodes are statistical support values for bootstrap proportions. The scale bar is in expected substitutions/site. **g** Phylogenetic tree based on mt genome data: Topology 7 with 13 concatenated genes at amino acid codification (protein-coding genes). Maximum-likelihood tree was reconstructed using the best fit evolutionary model for the concatenated matrix. Numbers at nodes are statistical support values for bootstrap proportions. The scale bar is in expected substitutions/site. **h** Phylogenetic tree based on mt genome data: Topology 8 with 13 concatenated genes at amino acid codification (protein-coding genes) implemented GBlock to trim the alignment. Maximum-likelihood tree was reconstructed using the best fit evolutionary model for the concatenated matrix. Numbers at nodes are statistical support values for bootstrap proportions. The scale bar is in expected substitutions/site. **i** Phylogenetic tree based on mt genome data: Topology 9 with 13 concatenated genes at amino acid codification (protein-coding genes). Bayesian tree was reconstructed using CAT-GTR evolutionary model for concatenated matrix. Numbers at nodes are statistical support values for bootstrap proportions. The scale bar is in expected substitutions/site. **j** Phylogenetic tree based on mt genome data: Topology 10 with 13 concatenated genes at amino acid codification (protein-coding genes) implemented GBlock to trim the alignment. Bayesian tree was reconstructed using CAT-GTR evolutionary model for concatenated matrix. Numbers at nodes are statistical support values for bootstrap proportions. The scale bar is in expected substitutions/site. **k** Phylogenetic tree based on mt genome data: Topology 11 with 13 concatenated genes at amino acid codification (protein-coding genes). Maximum-likelihood tree was reconstructed using mixture evolutionary model for concatenated matrix. Numbers at nodes are statistical support values for bootstrap proportions. The scale bar is in expected substitutions/site. **l** Phylogenetic tree based on mt genome data: Topology 12 with 13 concatenated genes at amino acid codification (protein-coding genes) implemented GBlock to trim the alignment. Maximum-likelihood tree was reconstructed using mixture evolutionary model for concatenated matrix. Numbers at nodes are statistical support values for bootstrap proportions. The scale bar is in expected substitutions/site.

Additional file 6: Figure S2. Phylogenetic tree based on nuclear ribosomal cluster. Maximum-Likelihood tree was reconstructed using the best fit evolutionary model for the concatenated matrix. Numbers at nodes are statistical support values for bootstrap proportions. The scale bar is in expected substitutions/site. The specimens sequenced in this study are highlighted in bold font with their respective GenBank access number in parentheses.

Additional file 7: Figure S3. a Biogeographic hypothesis using Biogeographic hypothesis using BioGeoBEARS DEC on garrapatas M0_unconstrained ancstates: global optim, 5 areas max. d = 0.0024; e = 0; j = 0; LnL = − 71.43. **b** Biogeographic hypothesis using BioGeoBEARS DEC+J on garrapatas M0_unconstrained ancstates: global optim, 5 areas max. d = 0.0018; e = 0; j = 0.0116; LnL = − 66.07. **c** Biogeographic hypothesis using BioGeoBEARS DIVALIKE on Psychotria M0_unconstrained ancstates: global optim, 5 areas max. d = 0.0028; e = 0; j = 0; LnL = − 69.79. **d** Biogeographic hypothesis using BioGeoBEARS DIVALIKE+J on Psychotria M0_unconstrained ancstates: global optim, 5 areas max. d = 0.0019; e = 0; j = 0.0104; LnL = − 66.16. Note: In all scenarios (**a**–**d**) five stages were assessed, each of them indicated with its respective abbreviation as follows: Nearctic, NE; Neotropic, NO; Australia, AU; Afrotropic, AF; Indomalayan, IN.

Acknowledgements

All laboratory work was conducted in and with the support of the Molecular Systematics Lab (https://www.mncn.csic.es/es/investigación/servicios-cientifico-tecnicos/laboratorio-de-sistematica-molecular) of MNCN-CSIC. Computing was conducted on the Smithsonian High Performance Cluster (https://doi.org/https://doi.org/10.25572/SIHPC). Many thanks to the Comunidad de Madrid for Atracción de Talento contract (REFF 2019-T2/AMB-13166) of JEU.

Author contributions

JEU, LRC, SN and SCB contributed to the conceptualization and main investigation. SN, FRP and SCB provided biological material. JEU, ACP and SK generated the molecular data. JEU and SP did the formal analyses. JEU, SN and SCB wrote the original draft. JEU administered and supervised the project. All authors have written, reviewed, edited and agreed to publish the final version of the manuscript.

Funding

This study was supported by Atracción Talento de la Comunidad de Madrid Fellowship Program (REFF 2019- T2/ AMB-13166).

Availability of data and materials

GenBank accession numbers generated in this study are available in Additional file 1: Table S1 and Additional file 7: Fig. S2.

Declarations

Ethics approval and consent to participate
Not applicable.

Competing interests
The authors declare that they have no competing interests.

Consent for publication
Not applicable.

Author details
[1]Biodiversity and Evolutionary Biology Department (BEBD), Museo Nacional de Ciencias Naturales (MNCN-CSIC), Madrid, Spain. [2]Invertebrate Zoology Department, National Museum of Natural History, Smithsonian Institution, Washington, DC, USA. [3]Department of Parasitology, School of Chemistry and Molecular Biosciences, The University of Queensland, Brisbane, QLD, Australia. [4]Estación Experimental Agropecuaria Rafaela (EEA Rafaela), Instituto Nacional de Tecnología Agropecuaria, Santa Fe, Argentina. [5]Department of Natural Sciences and Environmental Health, Faculty of Natural Sciences and Maritime Sciences of Technology, University of South-Eastern, Bø i Telemark, Norway. [6]Grupo de Investigación Evolución, Sistemática y Ecología Molecular (GIESEMOL), Facultad de Ciencias Básicas, Universidad del Magdalena, Santa Marta, Colombia. [7]Grupo de Investigación en Genética, Biodiversidad y Manejo de Ecosistemas (GEBIOME), Departamento de Ciencias Biológicas, Facultad de Ciencias Exactas y Naturales, Universidad de Caldas, Calle 65 No. 26-10, 170004 Manizales, Caldas, Colombia. [8]Epidemiology, Parasites and Vectors, Agricultural Research Council–Onderstepoort Veterinary Research, Onderstepoort, South Africa. [9]Department of Life and Consumer Sciences, University of South Africa, Pretoria, South Africa. [10]CSIRO Health and Biosecurity, Canberra, ACT, Australia.

Received: 2 October 2023 Accepted: 11 January 2024
Published online: 18 March 2024

References

1. Sonenshine DE, Roe RM. External and internal anatomy of ticks. Biol Ticks. 2014;1:74–98.
2. Jongejan F, Uilenberg G. The global importance of ticks. Parasitology. 2014;129:S3–14.
3. Piesman J, Eisen L. Prevention of tick-borne diseases. Annu Rev Entomol. 2008;53:323–43.
4. Magnarelli LA. Global importance of ticks and associated infectious disease agents. Clin Microbiol Newsl. 2009;31:33–7.
5. Gulia-Nuss M, Nuss AB, Meyer JM, Sonenshine DE, Roe RM, Waterhouse RM, et al. Genomic insights into the *Ixodes scapularis* tick vector of Lyme disease. Nat Commun. 2016;7:10507.
6. Guglielmone AA, Nava S, Robbins RG. Geographic distribution of the hard ticks (Acari: Ixodida: Ixodidae) ofthe world by countries and territories. Zootaxa. 2023:5251;1–274.
7. Mans BJ, Featherson J, Kvas M, Pillay KA, de Klerk D, Pienaar R, et al. Argasid and ixodid systematics: implications for soft tick evolution and systematics, with a new argasid species list. Ticks Tick-borne Dis. 2019;10:219–40.
8. Guglielmone AA, Nava S, Robbins RG. Neotropical Hard Ticks (Acari: Ixodida: Ixodidae). Berlin/Heidelberg: Springer International Publishing; 2021.
9. Hoogstraal H, Aeschlimann A. Tick-host specificity. Bul Soc Entomol Suisse. 1982;55:5–32.
10. Filippova NA. Classification of the subfamily Amblyomminae (Ixodidae) in connection with reinvestigation of chaetotaxy of the anal valve. Parazitologiâ. 1994;28:3–12.
11. Dobson SJ, Barker SC. Phylogeny of the hard ticks (Ixodidae) inferred from 18S rRNA indicates that the genus *Aponomma* is paraphyletic. Mol Phylogenet Evol. 1999;11:288–95.
12. Kaufman TS. A revision of the genus *Aponomma* Neumann, 1899 (Acarina: Ixodidae). Dissertation. College Park: University of Maryland; 1972.
13. Klompen JSH, Dobson SJ, Barker SC. A new subfamily, Bothriocrotninae n. subfam., for the genus *Bothriocroton* Keirans, King & Sharrad, 1994 status amend. (Ixodida: Ixodidae), and the synonymy of *Aponomma* Neumann, 1899 with *Amblyomma* Koch, 1844. Syst Parasitol. 2002;53:101–7
14. Barker SC, Burger TD. Two new genera of hard ticks, *Robertsicus* n. gen. and *Archaeocroton* n. gen., and the solution to the mystery of Hoogstraal's and Kaufman's "primitive" tick from the Carpathian Mountains. Zootaxa. 2018;4500(4):543–52.
15. Hornok S, Kontschán J, Takács N, Chaber AL, Halajian A, Abichu G, et al. Molecular phylogeny of *Amblyomma exornatu*m and *Amblyomma transversale*, with reinstatement of the genus Africaniella (Acari: Ixodidae) for the latter. Ticks Tick-borne Dis. 2020;11:101494.
16. Kelava S, Mans BJ, Shao R, Barker D, Teo EJ, Chatanga E, et al. Seventy-eight entire mitochondrial genomes and nuclear rRNA genes provide insight into the phylogeny of the hard ticks, particularly the *Haemaphysalis* species, *Africaniella transversale* and *Robertsicus elaphensis*. Ticks Tick-borne Dis. 2023;14:102070.
17. Estrada-Peña A, Venzal JM, Mangold AJ, Cafrune MM, Guglielmone AA. The *Amblyomma maculatum* Koch, 1844 (Acari: Ixodidae: Amblyomminae) tick group: diagnostic characters, description of the larva of *A. parvitarsum* Neumann, 1901, 16S rDNA sequences, distribution and hosts. Syst. Parasitol. 2005;60:99–112.
18. Marrelli MT, Souza LF, Marques RC, Labruna MB, Matioli SR, Tonon AP, et al. Taxonomic and phylogenetic relationships between neotropical species of ticks from genus *Amblyomma* (Acari: Ixodidae) inferred from second internal transcribed spacer sequences of rDNA. J Med Entomol. 2007;44:222–8.
19. Nava S, Mangold AJ, Mastropaolo M, Venzal JM, Oscherov EB, Guglielmone AA. *Amblyomma boeroi* n.sp. (Acari: Ixodidae), a parasite of the Chacoan peccary *Catagonus wagneri* (Rusconi) (Artiodactyla: Tayassuidae) in Argentina. Syst Parasitol. 2009;73:161–74.
20. Beati L, Nava S, Burkman EJ, Barros-Battesti DM, Labruna MB, Guglielmone AA, et al. *Amblyomma cajennense* (Fabricius, 1787)(Acari: Ixodidae), the Cayenne tick: phylogeography and evidence for allopatric speciation. BMC Evol Biol. 2013;13:1–20.
21. Lado P, Nava S, Labruna MB, Szabo MP, Durden LA, Bermudez S, et al. *Amblyomma parvum* Aragão, 1908 (Acari: Ixodidae): phylogeography and systematic considerations. Ticks Tick-borne Dis. 2016;7:817–27.
22. Lado P, Nava S, Mendoza-Uribe L, Caceres AG, Delgado-De La Mora J, Licona-Enriquez JD, et al. The *Amblyomma maculatum* Koch, 1844 (Acari: Ixodidae) group of ticks: phenotypic plasticity or incipient speciation?. Parasit Vectors. 2018;11:1–22.
23. Seabolt MH. Biogeographical patterns in the hard-tick genus *Amblyomma* Koch 1844 (Acari: Ixodidae). Dissertation. Statesboro: Georgia Southern University; 2016.
24. Beati L, Klompen H. Phylogeography of ticks (Acari: Ixodida). Annu Rev Entomol. 2019;64:379–97.
25. Uribe JE, Nava S, Murphy KR, Tarragona EL, Castro LR. Characterization of the complete mitochondrial genome of *Amblyomma ovale*, comparative analyses and phylogenetic considerations. Exp Appl Acarol. 2020;81:421–39.
26. Santodomingo A, Uribe JE, Lopez G, Castro LR. Phylogenetic insights into the genus *Amblyomma* in America, including the endangered species *Amblyomma albopictum*, *Amblyomma macfarlandi*, and *Amblyomma usingeri*. Int J Acarol. 2021;47:427–35.
27. Kelava S, Mans BJ, Shao R, Moustafa MAM, Matsuno K, Takano A, et al. Phylogenies from mitochondrial genomes of 120 species of ticks: insights into the evolution of the families of ticks and of the genus *Amblyomma*. Ticks Tick-borne Dis. 2021;12:101577.
28. Cotes-Perdomo AP, Nava S, Castro LR, Rivera-Paéz FA, Cortés-Vecino JA, Uribe JE. Phylogenetic relationships of the *Amblyomma cajennense* complex (Acari: Ixodidae) at mitogenomic resolution. Ticks Tick-borne Dis. 2023;14:102125.
29. Santos Dias JAT. Nova contribucao para o estudo da sistemática do género *Amblyomma* Koch, 1844 (Acarina-Ixodoidea). Garcia de Orta Ser Bot. 1993;9:11–9.
30. Camicas JL, Hervy JP, Adam F, Morel PC. Les tiques du monde (Acarida, Ixodida). Nomenclature, stades décrits, hôtes, répartition. ORSTOM. 1998;233.
31. Barker SC, Kelava S. What have we learned from the first 600 mitochondrial genomes of Acari? Zoosymposia. 2002;22:33–4.

32. Kneubehl AR, Muñoz-Leal S, Filatov S, de Klerk DG, Pienaar R, Lohmeyer KH, et al. Amplification and sequencing of entire tick mitochondrial genomes for a phylogenomic analysis. Sci Rep. 2022;12:19310.
33. Folmer O, Black M, Hoeh W, Lutz R, Vrijenhoek R. DNA primers for amplification of mitochondrial cytochrome *c* oxidase subunit I from diverse metazoan invertebrates. Mol Mar Biol Biotechnol. 1994;3:294–9.
34. Andrews S. FastQC. 2010. http://www.bioinformatics.babraham.ac.uk/projects/fastqc/.
35. Bolger AM, Lohse M, Usadel B. Trimmomatic: a flexible trimmer for Illumina sequence data. Bioinformatics. 2014;30:2114–20.
36. Prjibelski A, Antipov D, Meleshko D, Lapidus A, Korobeynikov A. Using SPAdes *de novo* assembler. Curr Protoc Bioinformatics. 2020;70:e102.
37. Bushmanova E, Antipov D, Lapidus A, Prjibelski AD. rnaSPAdes: a de novo transcriptome assembler and its application to RNA-Seq data. GigaScience. 2019;8:giz100.
38. Altschul SF, Madden TL, Schäffer AA, Zhang J, Zhang Z, Miller W, et al. Gapped BLAST and PSI-BLAST: a new generation of protein database search programs. Nucleic Acids Res. 1997;25:3389–402.
39. Bernt M, Donath A, Jühling F, Externbrink F, Florentz C, Fritzsch G, et al. MITOS: improved de novo metazoan mitochondrial genome annotation. Mol Phylogenetics Evol. 2013;69:313–9.
40. Boore JL, Macey JR, Medina M. Sequencing and comparing whole mitochondrial genomes of animals. Meth Enzymol. 2005;395:311–48.
41. Abascal F, Zardoya R, Telford MJ. TranslatorX: multiple alignment of nucleotide sequences guided by amino acid translations. Nucleic Acids Res. 2010;38:7–13.
42. Katoh K, Kuma KI, Toh H, Miyata T. MAFFT version 5: improvement in accuracy of multiple sequence alignment. Nucleic Acids Res. 2005;33:511–8.
43. Katoh K, Rozewicki J, Yamada KD. MAFFT online service: multiple sequence alignment, interactive sequence choice and visualization. Brief Bioinformatics. 2019;20:1160–6.
44. Felsenstein J. Journal of molecular evolution evolutionary trees from DNA sequences: a maximum likelihood approach. J Mol Evol. 1981;17:368–76.
45. Rannala B, Yang Z. Probability distribution of molecular evolutionary trees: a new method of phylogenetic inference. J Mol Evol. 1996;43:304–11.
46. Yang Z, Rannala B. Bayesian phylogenetic inference using DNA sequences: a Markov Chain Monte Carlo method. Mol Biol Evol. 1997;14:717–24.
47. Ronquist F, Huelsenbeck JP. MrBayes 3: Bayesian phylogenetic inference under mixed models. Bioinformatics. 2003;19:1572–4.
48. Lartillot N, Lepage T, Blanquart S. PhyloBayes 3: a Bayesian software package for phylogenetic reconstruction and molecular dating. Bioinformatics. 2009;25:2286–8.
49. Lartillot N, Philippe H. A Bayesian mixture model for across-site heterogeneities in the amino-acid replacement process. Mol Biol Evol. 2004;21:1095–109.
50. Rambaut A, Drummond AJ, Xie D, Baele G, Suchard MA. Posterior summarization in Bayesian phylogenetics using tracer 1.7. Syst Biol. 2018;67:901–4.
51. Schwarz D. Estimating the dimension of a model. Ann Stat. 1978;6:461–4.
52. Kalyaanamoorthy S, Minh BQ, Wong TKF, von Haeseler A, Jermiin LS. ModelFinder: fast model selection for accurate phylogenetic estimates. Nat Methods. 2017;14:587–9.
53. Bouckaert R, Heled J, Kühnert D, Vaughan T, Wu CH, Xie D, et al. BEAST 2: a software platform for Bayesian evolutionary analysis. PLoS Comput Biol. 2014;10:e1003537.
54. Matzke NJ. Model selection in historical biogeography reveals that founder-event speciation is a crucial process in island clades. Syst Biol. 2014;63:951–970.
55. Ree RH, Smith SA. Maximum likelihood inference of geographic range evolution by dispersal, local extinction, and cladogenesis. Syst Biol. 2008;57:4–14.
56. Ree RH, Sanmartín I. Conceptual and statistical problems with the DEC+J model of founder-event speciation and its comparison with DEC via model selection. J Biogeogr. 2018;45:741–9.
57. Wang T, Zhang S, Pei T, Yu Z, Liu J. Tick mitochondrial genomes: structural characteristics and phylogenetic implications. Parasit Vectors. 2019;12:451.
58. Soares JF, Labruna MB, de Amorim DB, Baggio-Souza V, Fagundes-Moreira R, Girotto-Soares A, et al. Description of *Amblyomma monteiroae* n. sp.(Acari: Ixodidae), a parasite of the great horned owl (Strigiformes: Strigidae) in southern Brazil. Ticks Tick-borne Dis. 2023;14:102239.
59. Barker SC, Walker AR, Campelo D. A list of the 70 species of Australian ticks; diagnostic guides to and species accounts of *Ixodes holocyclus* (paralysis tick), *Ixodes cornuatus* (southern paralysis tick) and *Rhipicephalus australis* (Australian cattle tick); and consideration of the place of Australia in the evolution of ticks with comments on four controversial ideas. Int J Parasitol. 2014;44:941–53.
60. Medlin JS, Cohen JI, Beck DL. Vector potential and population dynamics for *Amblyomma inornatum*. Ticks Tick-borne Dis. 2015;6:463–72.
61. Nava S, Venzal JM, González-Acuña D, Martins TF, Guglielmone AA. Ticks of the Southern Cone of America: Diagnosis, Distribution and Hosts with Taxonomy, Ecology and Sanitary Importance. London: Elsevier/Academic Press; 2017.
62. Krawczak FS, Martins TF, Oliveira CS, Binder LC, Costa FB, Nunes PH, et al. *Amblyomma yucumense* n. sp. (Acari: Ixodidae), a parasite of wild mammals in Southern Brazil. J Med Entomol. 2015;52(1):28–37.
63. Amarga AKS, Supsup CE, Tseng HY, Kwak ML, Lin SM. The Asian turtle tick *Amblyomma geoemydae* Cantor, 1847 (Acari: Ixodidae) in the Philippines: first confirmed local host and locality with a complete host index. Ticks Tick-borne Dis. 2022;13:101958.
64. Kwak ML, Kuo CC, Chu HT.2020). First record of the sea snake tick *Amblyomma nitidum* Hirst and Hirst, 1910 (Acari: Ixodidae) from Taiwan. Ticks Tick-Borne Dis. 2020;11(3):101383.
65. Kemp DH, Wilson N. The occurrence of *Amblyomma cyprium cyprium* (Acari: Ixodidae) in Australia, with additional records from the southwest Pacific. Pac Insects. 1979;21:224–6.
66. Cotes-Perdomo AP, Sánchez-Vialas A, Thomas R, Jenkins A, Uribe JE. New insights into the systematics of the Afrotropical *Amblyomma marmoreum* complex (Acari, Ixodidae) and a novel *Rickettsia africae* strain using morphological and metagenomic approaches. bioRxiv. 2023;08.
67. Nava S, Guglielmone AA, Mangold AJ. An overview of systematics and evolution of ticks. Front Biosci. 2009;14:2857–77.
68. Grimaldi DA, Engel MS, Nascimbene PC. Fossiliferous cretaceous amber from Myanmar (Burma): Its rediscovery, biotic diversity, and paleontological significance. Am Mus Novit. 2002;3361:1–71.
69. Morrone JJ. Biogeographical regionalisation of the Neotropical region. Zootaxa. 2014;3782:1–110.
70. Hewitt G. The genetic legacy of the Quaternary ice ages. Nature. 2000;405:907–13.
71. Raven PH, Gereau RE, Phillipson PB, Chatelain C, Jenkins CN, Ulloa-Ulloa C. The distribution of biodiversity richness in the tropics. Sci Adv. 2020;6:eabc6228.
72. Sanmartíin I, Ronquist F. Southern hemisphere biogeography inferred by event-based models: plant versus animal patterns. Syst Biol. 2004;216–243.
73. Veevers JJ. Gondwanaland from 650–500 Ma assembly through 320 Ma merger in Pangea to 185–100 Ma breakup: supercontinental tectonics via stratigraphy and radiometric dating. Earth-Sci Rev. 2004;68:1–132.
74. Hill ED. Salticidae of the Antarctic land bridge. Peckhamia. 2009;76:1–14.
75. Yanbin S. A paleoisthmus linking southern South America with the Antarctic Peninsula during Late Cretaceous and Early Tertiary. Sci China Earth Sci. 1998;41:225–9.
76. Sanmartín I, Enghoff H, Ronquist F. Patterns of animal dispersal, vicariance and diversification in the Holarctic. Biol J Linn Soc. 2001;73:345–90.
77. de Porta J. La formación del istmo de Panamá. Su incidencia en Colombia. Rev Acad Colomb Cienc. 2003;27:191–216.
78. Marshall JS. Geomorphology and physiographic provinces of Central America. In: Bundschuh J, Alvarado G, editors. Central America: geology, resources, and natural hazards. London: Taylor & Francis; 2007. p. 75–121.
79. Morrone JJ. Halffter's Mexican transition zone (1962–2014), cenocrons and evolutionary biogeography. Zool Syst Evol Res. 2015;53:249–57.
80. Jeyaprakash J, Hoy MA. First divergence time estimate of spiders, scorpions, mites and ticks (subphylum: Chelicerata) inferred from mitochondrial phylogeny. Exp Appl Acarol. 2009;47:1–18.
81. Chitimia-Dobler L, De Araujo BC, Ruthensteiner B, Pfeffer T, Dunlop JA. *Amblyomma birmitum* a new species of hard tick in Burmese amber. Parasitology. 2017;144:1441–8.
82. Klompen JSH, Black WC IV, Keirans JE, Norris DE. Systematics and biogeography of hard ticks, a total evidence approach. Cladistics. 2000;16:70–102.

83. Barker D, Seeman OD, Barker SC. The development of tick taxonomy and systematics in Australia and contributors and with comments on the place of Australasia in the study of the phylogeny and evolution of the ticks. Syst Appl Acarol. 2021;26:1793–832.
84. Zwickl DJ, Hillis DM. Increased taxon sampling greatly reduces phylogenetic error. Syst Biol. 2002;51:588–98.
85. Heath TA, Hedtke SM, Hillis DM. Taxon sampling and the accuracy of phylogenetic analyses. J Syst Evol. 2008;46:239.

Publisher's Note